

ACTIVATION ENERGY OF CRYSTALLIZATION AND ENTHALPY RELEASED OF $\text{Se}_{90}\text{In}_{10-x}\text{Sb}_x$ ($x=0, 2, 4, 6, 8, 10$) CHALCOGENIDE GLASSES

PRAVEEN K. JAIN^{a*}, DEEPIKA^b, K.S. RATHORE^b, NIDHI JAIN^c,
N.S. SAXENA^b

^a*Department of Physics, Indian Institute of Technology Roorkee, Roorkee-Utranchal, India*

^b*5, 6 Vigyan Bhawan, University of Rajasthan, Jaipur-Rajasthan, India*

^c*Department of Physics, Institute of Technology & Management, Bhilwara-Rajasthan, India*

$\text{Se}_{90}\text{In}_{10-x}\text{Sb}_x$ ($x=0, 2, 4, 6, 8, 10$) chalcogenide glasses are prepared by melt quenching method. Devitrification characteristics of the alloys were investigated by using Differential Scanning Calorimetry (DSC). The glassy samples are scanned in DSC at various heating rates of 5, 10, 15, 20, 25, and 30 K/min. The dependence of on-set crystallization temperature (T_c) on heating rates as well as different concentration of Sb is studied. Using partial peak area analysis of the crystallization peak in the DSC thermograms, the volume fraction of the glass crystallized at various temperatures is evaluated. The crystallization data were analyzed with the Matusita and Sakka's method specifically suggested for non-isothermal crystallization. This method is used to calculate the activation energy of crystallization (E_c) and Avrami index (n) and hence the dimensionality of crystal growth. The variation of activation energy of crystallization (E_c) with heating rate and Sb concentration has also been studied. Thermal stability has been monitored through the calculation of the enthalpy released during crystallization (ΔH_c).

(Received January 17, 2009; accepted March 18, 2009)

Keywords: Chalcogenide glass, Activation energy of crystallization, DSC, Avrami index.

1. Introduction

Traditionally, solid-state physics has meant crystal physics. Solidity and crystallinity are considered as synonymous in text on condensed matter. Yet one of the most active fields of solid state research in recent years has been the study of solids that are not crystals, solids in which the arrangements of atoms lack the slightest vestige of long range order. The advances that have been made in the physics and chemistry of these materials, which are known as amorphous solids or glasses, have been widely appreciated within research community.

Recently, great attention has been given to chalcogenide glasses mainly due to their wide range of application in solid-state devices both in scientific and technological fields. Optical data storage based on laser induced amorphous to crystalline (a-c) phase transformation of chalcogenide glasses is an area with on going research activity [1]. Especially selenium (Se) based alloys exhibit a unique property of reversible transformation. This property makes these systems very useful in optical memory devices, X-ray imaging and photonics [2-6].

The structure of amorphous Se and the effect of alloying Indium (In) into Se have been carried out by workers and reported [5, 6] in the literature. These studies indicate that when In is incorporated to amorphous Se it is dissolved in the Se chains to satisfy its coordination

* Corresponding author: praveenjain.spsl@gmail.com

requirements and to form a crosslink structure, which retards the crystallization probability and enhance thermal stability. Besides, it is also found that the optical band gap of Se-In is of the order of 1.3 eV at 300 K, which is close to the theoretical optimum value for solar energy conversion [7]. In spite of that, these alloys are still found to have low glass transition and crystallization temperature and hence their physical properties may deteriorate with temperature and time during use. The addition of third element, like Sb, to Se-In alloys will expand the glass forming region and create compositional and configurationally disorder, which offer ample possibilities for controlling the desired thermal properties by means of changing the chemical composition [8].

2. Experimental details

Glassy alloys of $\text{Se}_{90}\text{In}_{10-x}\text{Sb}_x$ ($x=0, 2, 4, 6, 8, 10$) are prepared by melt quenching technique. High purity (99.999 %) materials were weighed according to their atomic percentage and were sealed in quartz ampoules (length 10.5 cm and 8 mm internal diameter) with a vacuum of 10^{-5} Torr. The sealed ampoules are kept inside the furnace where the temperature was raised to 900 °C at the rate of 3 to 4 K/min. The ampoules were frequently rocked for 15 hours at maximum temperature to make the melt homogeneous. The molten sample was then quenched in ice-cooled water. The ingot of so produced glassy sample was taken out of ampoule and then grinded gently in mortar and pestle to obtain powder form.

The amorphous nature of the alloy was ascertained through X-ray diffraction pattern of the samples using diffractometer with FeK_α -radiation source ($\lambda = 1.93 \text{ \AA}$). Fig. 1 shows the XRD pattern $\text{Se}_{90}\text{In}_2\text{Sb}_8$ glass at room temperature. Absence of any sharp peak confirms the formation of glass.

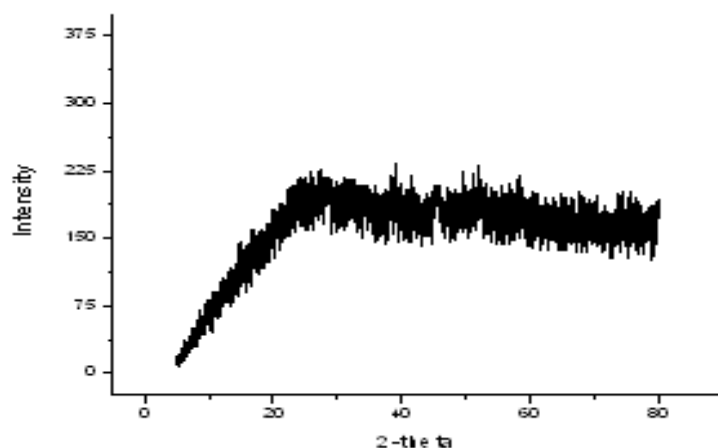


Fig. 1 XRD pattern of $\text{Se}_{90}\text{In}_2\text{Sb}_8$ chalcogenide glass at room temperature.

Differential Scanning Calorimetry (DSC) Rigaku Model 8230 is used to measure the caloric manifestation of the phase transformation and to study the crystallization kinetics under non-isothermal condition. The accuracy of heat flow measurement is $\pm 0.01 \text{ mW}$ and the temperature precision as determined by the microprocessor of the thermal analyzer is $\pm 0.1 \text{ K}$. The DSC runs have been taken at six different heating rates i.e. 5, 10, 15, 20, 25, and 30 K/min on accurately weighed samples taken in aluminum pans. The temperature range covered in DSC was from room temperature to 250 °C.

3. Results and discussion

Fig. 2 shows the typical DSC thermograms of $\text{Se}_{90}\text{In}_{10-x}\text{Sb}_x$ ($x=0, 2, 4, 6, 8, 10$) glasses at the heating rate of 10 K/min. The endothermic peak of glass transition and exothermic peak of crystallization have been clearly observed in the Fig.2. The on-set crystallization temperature T_c , has been defined as temperature corresponding to the intersection of two linear portion adjoining

the transition elbow of the DSC trace in the exothermic direction. The values of on-set crystallization temperature (T_c) at different heating rates for all the compositions are given in the Table 1. It is found that on-set crystallization temperature increases as Sb concentration increases upto 4 atomic weight % and further addition of Sb reduces the crystallization temperature.

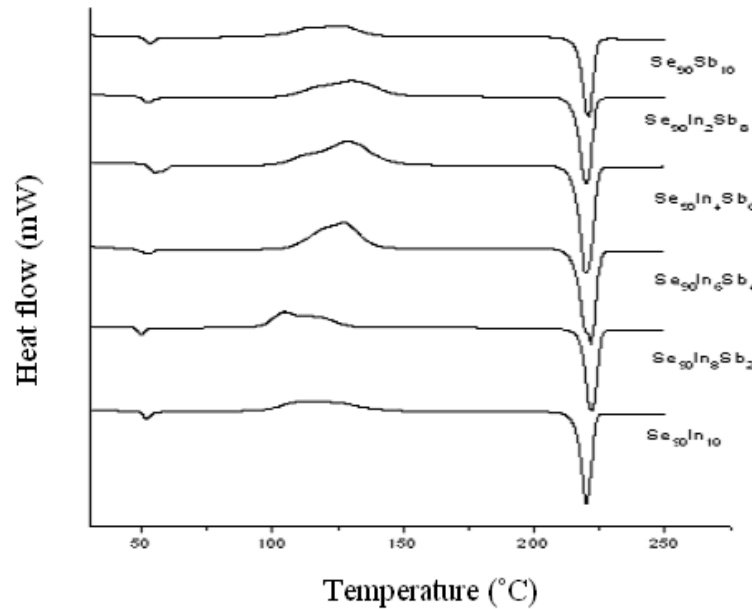


Fig. 2. DSC traces of $Se_{90}In_{10-x}Sb_x$ ($x=0, 2, 4, 6, 8, 10$) chalcogenide glass at 10 K/min heating rates

Table1. On-set crystallization temperature T_c (K) calculated from DSC result.

Heating Rate	5 K/min	10 K/min	15 K/min	20 K/min	25 K/min	30 K/min
Sample						
$Se_{90}In_{10}$	360.5	367.8	372.1	375.4	377.6	379.8
$Se_{90}In_8Sb_2$	367.3	374.6	378.4	381.9	384.8	386.8
$Se_{90}In_6Sb_4$	370.9	377.3	382.1	384.4	387.2	390.2
$Se_{90}In_4Sb_6$	368.4	375.2	379.4	382.7	385.8	387.8
$Se_{90}In_2Sb_8$	367.5	373.9	378.6	382.3	384.9	386.8
$Se_{90}Sb_{10}$	364.0	371.4	376.2	378.6	381.4	383.5

The dependence of on-set crystallization temperature (T_c) on the heating rate (α) is given by the empirical relation that has been suggested by Lasocka [9] and has the form

$$T_c = A_c + B_c \ln(\alpha) \quad (1)$$

where A_c and B_c are constants.

The plots of $\ln(\alpha)$ vs T_c for $\text{Se}_{90}\text{In}_{10-x}\text{Sb}_x$ ($x=0, 2, 4, 6, 8, 10$) glassy alloys are shown in Fig.3. The straight line shows the good validity of this relationship for the alloy. The calculated values of A_c and B_c are given in Table 2. In Table 2, A_c depict the crystallization temperature at a heating rate of 1 K/min while B_c are proportional to the time taken by the system to reduce its glass transition and crystallization temperature when its heating rate is lowered from 10 K/min to 1 K/min.

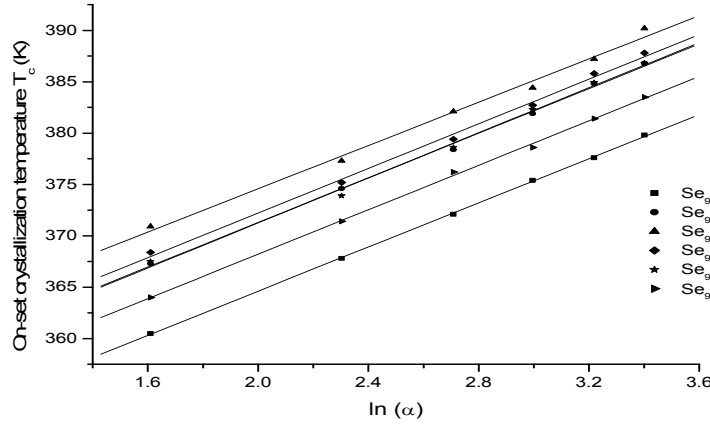


Fig. 3. $\ln(\alpha)$ vs T_c for $\text{Se}_{90}\text{In}_{10-x}\text{Sb}_x$ ($x=0, 2, 4, 6, 8, 10$) glassy alloys.

Table. 2 Calculated values of constants A_c and B_c for $\text{Se}_{90}\text{In}_{10-x}\text{Sb}_x$ ($x=0, 2, 4, 6, 8, 10$) chalcogenide glass.

Sample	A_c (K)	B_c (min)
$\text{Se}_{90}\text{In}_{10}$	343.13 ± 0.23	10.74 ± 0.09
$\text{Se}_{90}\text{In}_8\text{Sb}_2$	349.58 ± 0.73	10.86 ± 0.26
$\text{Se}_{90}\text{In}_6\text{Sb}_4$	353.51 ± 1.20	10.54 ± 0.43
$\text{Se}_{90}\text{In}_4\text{Sb}_6$	350.51 ± 0.88	10.86 ± 0.32
$\text{Se}_{90}\text{In}_2\text{Sb}_8$	349.33 ± 0.95	10.96 ± 0.34
$\text{Se}_{90}\text{Sb}_{10}$	346.58 ± 0.50	10.82 ± 0.18

The variation of T_c with composition at different heating rates for $\text{Se}_{90}\text{In}_{10-x}\text{Sb}_x$ ($x=0, 2, 4, 6, 8, 10$) is shown in Fig.4.

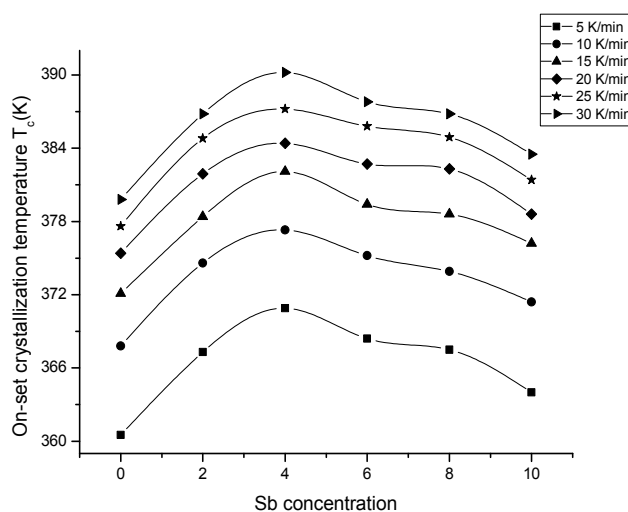


Fig. 4. Variation of on-set crystallization temperature T_c with Sb concentration at different heating rates

It has been indicated that in Se containing glass, there is a tendency to form polymerized network glasses and the homopolar bond is qualitatively suppressed [10]. The on-set crystallization temperature increases upto 4 at % of Sb and with further addition of Sb the chains as well as ring structures are affected and a decrease in T_c is observed, for further higher values of Sb concentration, T_c becomes almost constant as shown in Fig. 4. Moreover, at lower percentage of Sb the system contains $\text{SbSe}_{4/2}$ tetrahedral units dissolved in a matrix composed of Se chains. With the increases of Sb content, the glassy matrix becomes heavily cross-linked and the steric hindrance increases. The Se-Se bonds (bond energy 205.8 KJ/mol) will be replaced by Sb-Se bonds, which have a higher bond energy (214.2 KJ/mol). Hence the cohesive energy of the system increases with increasing Sb content. This results in the increase of the crystallization temperature. It is found that T_c is maximum at 4 at % of antimony (Sb). This composition can be considered as a critical composition at which the system becomes a chemically ordered alloy containing high-energy Sb-Se heteropolar bonds. Further addition of Sb favours the formation of Sb-Sb bonds (bond energy 176.4 KJ/mol) thus reducing the Sb-Se bond concentration. Thus the cohesive energy decreases results a decrease of T_c .

The kinetics of crystallization as a function of composition has been studied to aid our understanding of transformation that is encountered in the sample under consideration. The most successful and applicable theoretical model for crystallization studies is the one suggested by Johnson – Mehl - Avrami [11-13] (JMA). According to this model, the fraction, χ , of precursor that has been transformed into the product phase is given by

$$\chi = 1 - \exp(-Kt^n) \quad (2)$$

where n is the Avrami exponent and reflects the details of crystal growth. K is the effective overall reaction rate, which actually reflects the rate of crystallization and usually assigned Arrhenian temperature dependence,

$$K = K_0 \exp(-E_c/RT) \quad (3)$$

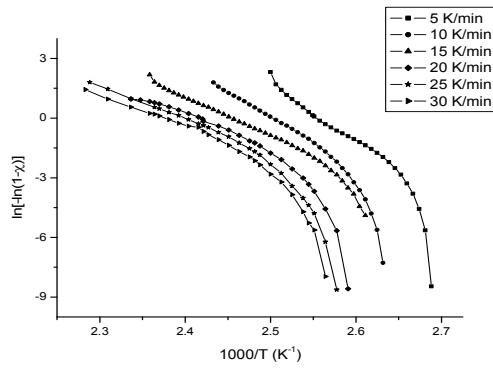
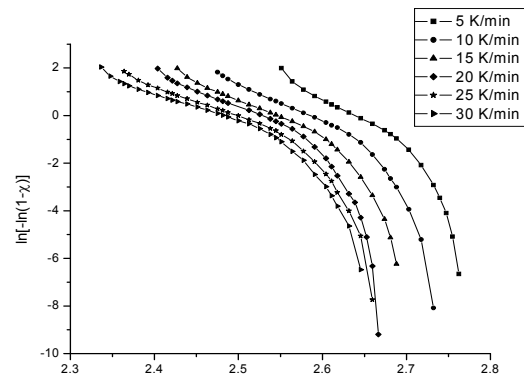
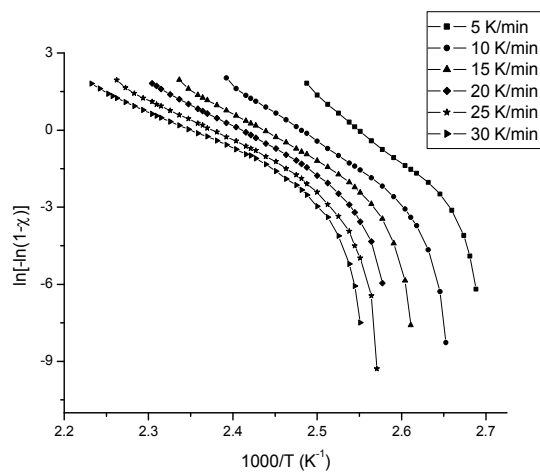
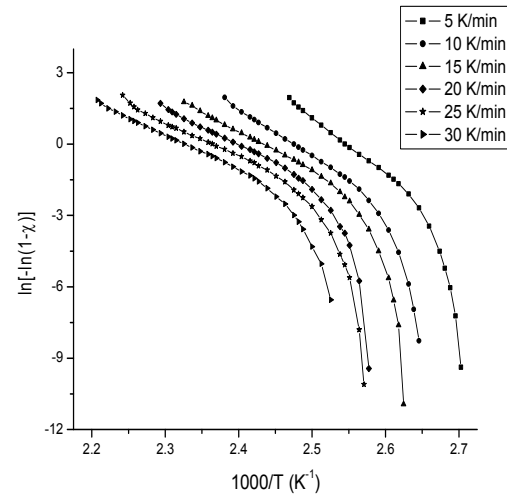
Here K_0 , the frequency factor, which indicates the number of attempts made by nuclei to overcome the energy barrier during crystallization. E_c is activation energy of crystallization.

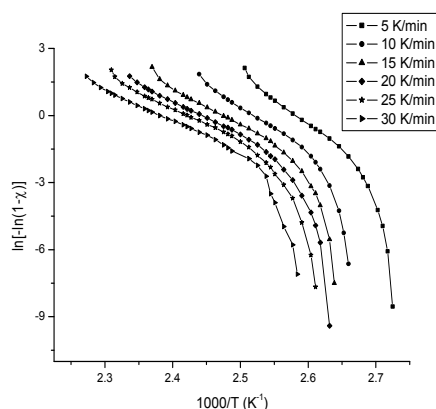
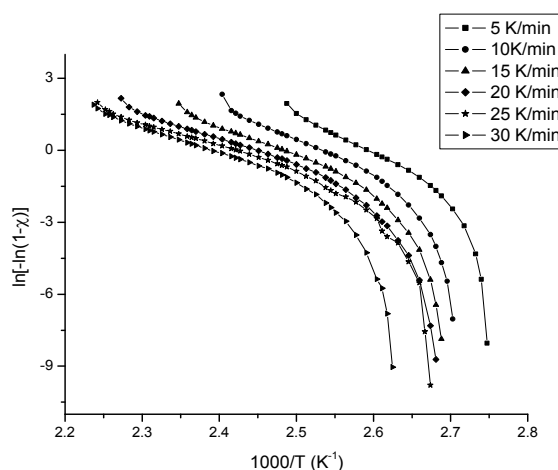
In the non-isothermal method, the crystallization fraction (χ) precipitated in the glass heated at constant rate, is related to the activation energy for crystallization (E_c), through the following expression given by Matusita et al. [14].

$$\ln[-\ln(1-\chi)] = -n \ln \alpha - 1.052mE_c/RT + \text{constant} \quad (4)$$

where m and n are integer or half integer numbers that depend on the growth mechanism and the dimensionality of the crystal. The parameter n can be written as $n=b+pm$ where $p=1$ for linear growth and $p=0.5$ for parabolic growth, $m=1, 2$ or 3 for one-, two-, or three-dimensional growth, $b=0$, $b<1$ and $b>1$ are chosen for no nucleation, decreasing nucleation and increasing nucleation rate, respectively. The volume fraction χ crystallized at any temperature T is given by $\chi = A_T/A$, where A is the total area of the exothermic peak between the on-set temperature T_c (i.e. the temperature from where crystallization starts) and temperature where the peaks end (i.e. crystallization is complete). A_T is the partial area of the exothermic peak between temperature T_c and T .

The plots of $\ln[-\ln(1-\chi)]$ against $1000/T$ at different fixed heating rates for all the glassy sample are shown in Fig.5 (a) to Fig. 5 (f), where it can be noticed that the curves have nearly the same slope over the most temperature range. At high temperature range or in the regions of large crystallized fractions, a deviation from linearity is shown for the different heating rates. Other chalcogenide glasses indicated a similar behavior [15-17]. This deviation is generally attributed to the saturation of nucleation sites in the final stage of crystallization or to restriction of crystal growth by the small size of the particles.

Fig.5 (a) $Se_{90}In_{10}$ Fig.5 (b) $Se_{90}In_8Sb_2$ Fig.5 (c) $Se_{90}In_6Sb_4$ Fig.5 (d) $Se_{90}In_4Sb_6$

Fig.5 (e) $Se_{90}In_2Sb_8$ Fig.5 (f) $Se_{90}Sb_{10}$

The values of activation energy obtained from the slop of the curves between $\ln[-\ln(1-\chi)]$ versus $1000/T$ at all the heating rates for $Se_{90}In_{10-x}Sb_x$ ($x=0,2,4,6,8,10$) chalcogenide glasses are listed in Table 3. From the Table 3, it is clear the activation energy depends on the heating rate and decreases as the heating rate increases. The average activation energy increases with the addition of Sb concentration and have the maximum value at 4 atomic % of Sb, more addition of Sb reduces the activation energy.

Table3. Calculated values of activation energy E_c (KJ/mol) obtained from Matusita's method

Heating rate	5 K/min	10 K/min	15 K/min	20 K/min	25 K/min	30 K/min
Sample						
$Se_{90}In_{10}$	112.57 ± 3.44	95.96 ± 1.39	88.42 ± 1.37	84.84 ± 1.43	73.62 ± 1.41	70.08 ± 1.15
$Se_{90}In_8Sb_2$	123.73 ± 3.80	114.24 ± 1.86	83.93 ± 0.55	85.59 ± 3.75	82.35 ± 2.87	76.49 ± 2.85
$Se_{90}In_6Sb_4$	146.12 ± 2.32	122.11 ± 0.95	103.78 ± 1.02	99.00 ± 1.13	92.49 ± 1.20	83.96 ± 1.21
$Se_{90}In_4Sb_6$	131.21 ± 1.23	112.13 ± 1.61	96.14 ± 1.84	88.21 ± 1.43	84.28 ± 1.56	80.83 ± 0.68
$Se_{90}In_2Sb_8$	125.44 ± 3.42	108.52 ± 2.24	88.87 ± 1.29	85.65 ± 1.41	80.10 ± 1.40	76.39 ± 1.04
$Se_{90}Sb_{10}$	119.54 ± 2.48	105.73 ± 2.82	89.21 ± 1.70	78.20 ± 1.40	75.99 ± 1.60	79.01 ± 1.25

The heating rate dependence of the activation energy determined by this method is also shown in Fig. 6 for $Se_{90}In_6Sb_4$ glassy sample. The observed heating rate dependence of the effective activation energy can be attributed to changes of nucleation and growth mechanism.

Sahay and Krishnan [18] have pointed out that a relationship between effective activation energy (E_c) and the heating rate (α) should be considered when analyzing kinetic data in some chalcogenide glasses and have suggested that the observed decrease in E_c as heating rate increases is due to an increase in free energy of the reactant and product phases which results in the reduction of the effective activation energy. It is also possible that this effect is a result of the temperature dependence of E_c .

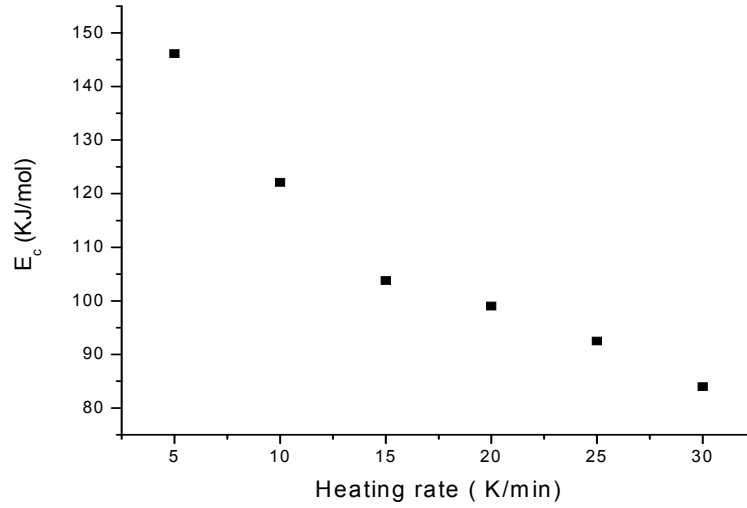


Fig. 6. Plot of heating rate versus activation energy of crystallization for $Se_{90}In_6Sb_4$ glass

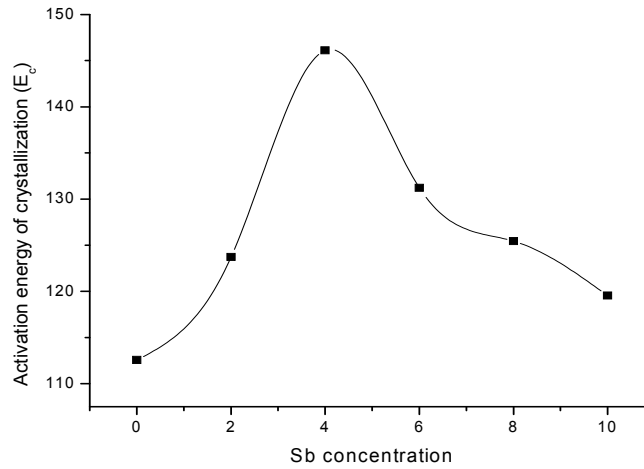
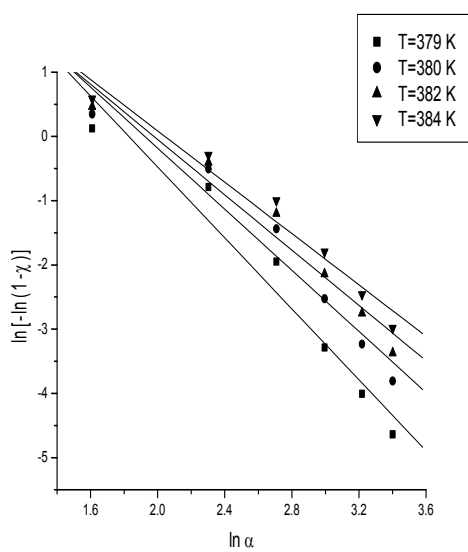
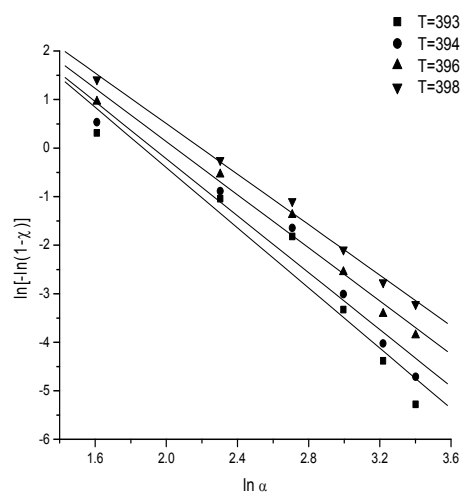
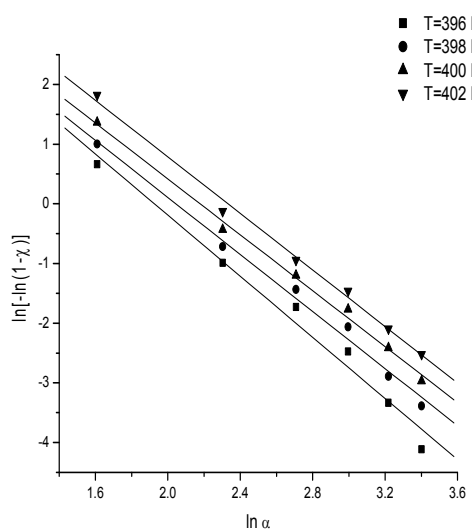
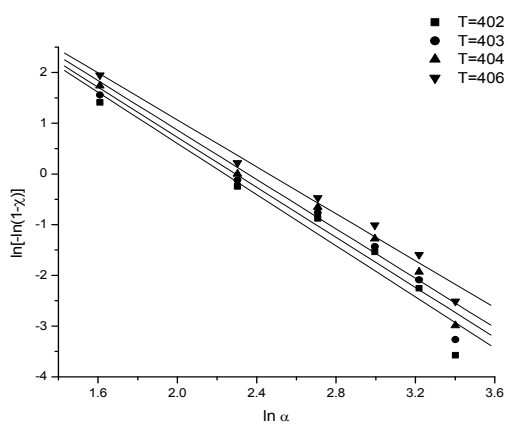


Fig. 7. E_c vs Sb concentration for $Se_{90}In_{10-x}Sb_x$ ($x=0, 2, 4, 6, 8, 10$) at heating rate 5 K/min.

The plots of $\ln [-\ln (1-\chi)]$ against $\ln \alpha$ at four different temperatures are shown in Fig 7(a) to Fig. 7(f). From the slope of this curve, the order of crystallization mechanism or Avrami index (n) can be obtained and observed average values are listed in Table 4.

Fig.7 (a) $\text{Se}_{90}\text{In}_{10}$ Fig.7 (b) $\text{Se}_{90}\text{In}_8\text{Sb}_2$ Fig.7 (c) $\text{Se}_{90}\text{In}_6\text{Sb}_4$ Fig.7 (d) $\text{Se}_{90}\text{In}_4\text{Sb}_6$

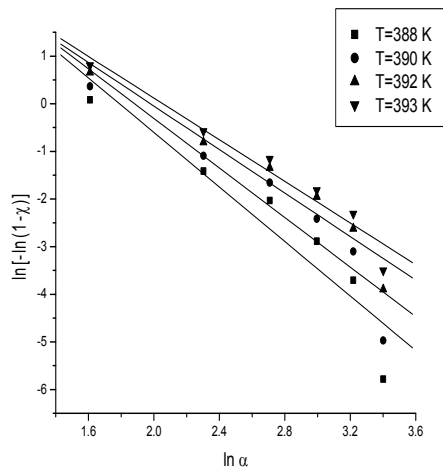
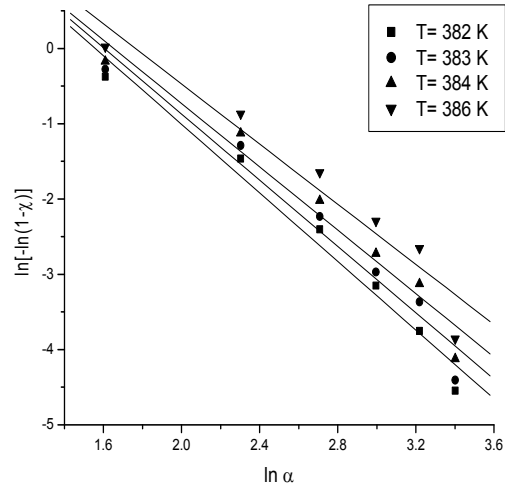
Fig.7 (e) $\text{Se}_{90}\text{In}_2\text{Sb}_8$ Fig.7 (f) $\text{Se}_{90}\text{Sb}_{10}$

Table 4: Values of Avrami index (n) and dimensionality of growth (m) of $\text{Se}_{90}\text{In}_{10-x}\text{Sb}_x$ ($x=0, 2, 4, 6, 8, 10$) chalcogenide glasses.

Sample	Avrami index (n)	Dimensionality of growth (m)
$\text{Se}_{90}\text{In}_{10}$	2.32 ± 0.25	1
$\text{Se}_{90}\text{In}_8\text{Sb}_2$	2.85 ± 0.25	2
$\text{Se}_{90}\text{In}_6\text{Sb}_4$	2.42 ± 0.12	1
$\text{Se}_{90}\text{In}_4\text{Sb}_6$	2.44 ± 0.23	1
$\text{Se}_{90}\text{In}_2\text{Sb}_8$	2.48 ± 0.38	1
$\text{Se}_{90}\text{Sb}_{10}$	2.15 ± 0.23	1

Measuring the total area under the exothermic peak, the experimental determination of enthalpy-released ΔH_c during crystallization process has been made

$$\Delta H_c = KA/M \quad (5)$$

where K is the instrument constant, which is found to be 1.12; A is the area under the crystallization peak and M is the mass of the sample. The value of ΔH_c at heating rate 15 K/min is plotted as a function of Sb content in Fig.8. From Fig. 8, it is clear that $\text{Se}_{90}\text{In}_6\text{Sb}_4$ glass has lowest value of ΔH_c , hence is the most stable among the whole series.

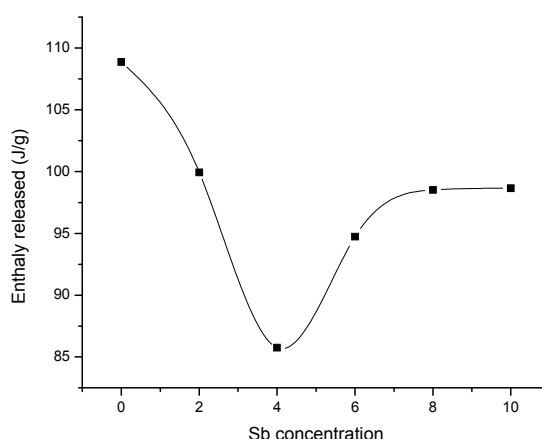


Fig. 8 Enthalpy released, ΔH_c , at heating rate 15 K/min, plotted as a function of Sb content

4. Conclusions

Based on the present study the following conclusion can be drawn:

1. The activation energy of crystallization decreases with increasing heating rate. This activation energy of crystallization increases as the Sb concentration increases up to 4 atomic weight percentages and further addition of Sb reduces it.
2. According to the Avrami theory of nucleation, the calculated values of the kinetic exponent n suggest two dimensional growth for $\text{Se}_{90}\text{In}_8\text{Sb}_2$ glassy sample while all other sample $\text{Se}_{90}\text{In}_{10-x}\text{Sb}_x$ ($x = 0, 4, 6, 8, 10$) have one dimensional growth.
3. Enthalpy released during crystallization decreases upto 4 atomic weight percentage of Sb and then further increases with Sb concentration. This suggests that $\text{Se}_{90}\text{In}_6\text{Sb}_4$ glass has most stable among the whole series.

References

- [1] N. Mehta, M.Zulfequar, A.Kumar, J. Optoelectron. Adv. Mat **6**, 441 (2004)
- [2] I.D. Aggarwal, J.S. Sanghera, J. Optoelectron. Adv. Mat. **4**, 665 (2002).
- [3] M. Mitkova, in Amorphous Semiconductors and Insulators, edited by P. Boolchand, World Scientific Press LTD, 2000, p. 813
- [4] S.R. Ovshinsky, in Non-Crystalline Materials for Optoelectronics, edited by G. Lucovsky and M. Popescu, INOE, 2004, p. 1.
- [5] Dessaur JH, Clarke HE. Xerography and Related Processes. Local, London, 1965.
- [6] Ovshinsky R. Phys Rev Lett **21**, 1450 (1986)
- [7] K.Singh, N.S.Saxena, O.N.Srivastava, D.Patidar, T.P.Sharma, Chalcogenide Letters **3**, 33(2006)
- [8] Kaur G., and Komatsu T., J. Mater. Sci., **36**, 4531(2001)
- [9] M. Lasocka, Matter. Sci. Eng. **23**, 173 (1973)
- [10] Rabinal, M.K., Ramesh Rao, N., and Mathur, P.C., J. Mater. Sci., **26**, 3433 (1991).
- [11] M.Avrami, J.Phys. Chem **7**, 212 (1939).
- [12] M.Avrami, J.Phys. Chem **8**, 212 (1940)
- [13] W.A. Johnson and R.F. Mehl, Trans.Am.Inst.Miner.Eng.**135**, 419 (1939).
- [14] K.Matusita, T.Konatsu, R.Yorota, J. Mater.Sci.**19**, 291 (1984).
- [15] M.A.Abdel-Rahim, M.M.Hafiz, A.M.Shamekh, Physica B**369**, 143 (2005)
- [16] S.N.Zhang, T.J.Zhu, X.B.Zhao, Physica B **403**, 3459 (2008)
- [17] N.Ziani, M.Belhadji, L. Heireche, Z. Bouchaour, M.Belbachir, Physica B **358**, 132 (2005)
- [18] S.S. Sahay, K. Krishnan, Physica B **348**, 310(2004)